N88-16649

# AEROACOUSTIC RESEARCH PROGRAMS AT THE ARMY AVIATION RESEARCH AND TECHNOLOGY ACTIVITY

Yung H. Yu,* Fredric H. Schmitz,† and H. Andrew Morse‡
Fluid Mechanics Division
Aeroflightdynamics Directorate
U.S. Army Research and Technology Activity (AVSCOM)
Moffett Field, California

## ABSTRACT

The Army rotorcraft aeroacoustic programs are reviewed, highlighting the theoretical and experimental progress made by Army researchers in the physical understanding of helicopter impulsive noise. The two impulsive noise sources addressed over this past decade are high-speed impulsive noise and blade-vortex interaction noise, both of which have had and will continue to have an increasing influence on Army rotorcraft design and operations. The advancements discussed are in the areas of in-flight data acquisition techniques, small-scale-model tests in wind tunnels, holographic interferometry/tomographic techniques, and the expanding capabilities of computational fluid dynamics in rotorcraft acoustic problems. Current theoretical prediction methods are compared with experimental data, and parameters that govern model scaling are established. The very successful cooperative efforts between the Army, NASA, and industry are also addressed.

## 1. INTRODUCTION

Noise generated by a helicopter has been a difficult scientific problem for many years. It has many different origins, most of which are related to aerodynamic phenomena around rotor blades and the fuselage. Over the past decades, many major analytical and experimental developments were made by the Army research efforts. Some of the most notable are comprehensive acoustic prediction codes for high-speed impulsive noise, an in-flight acoustic measurement technique, and a joint government/industry test program in a world-class anechoic wind tunnel. In many cases these developments led to the discovery of many important rotorcraft acoustic characteristics and aerodynamic phenomena related to impulsive noise. In the

*Division Chief, Fluid Mechanics, Aeroflightdynamics Directorate.
†Currently Division Chief, Full-Scale Aerodynamics Research Division, NASA Ames Research Center.
‡Senior Staff Scientist, Aeroflightdynamics Directorate.

following text, two different impulsive noise-generating mechanisms are reviewed; high-speed impulsive noise and blade-vortex interaction (BVI) noise.

## 2. HIGH-SPEED IMPULSIVE NOISE

Over the past 10 years, an in-flight method of gathering helicopter impulsive noise data has been developed by the Aeroflightdynamics Directorate (ARTA, AVSCOM) (ref. 1). A quiet, fixed-wing aircraft (OV-1C and later the YO-3A) was instrumented with microphones and flown in formation with the subject helicopter, as shown in figure 1. Because these aircraft are relatively quiet and the impulsive signals are intense, good-quality acoustic data were acquired. The major advantages of gathering data in this manner are (1) there are no ground reflections; (2) there are long and steady data samples; and (3) helicopter flight conditions and directivity profiles are easily explored. From data taken during high-speed level flight, a strong negative pressure peak, called high-speed impulsive noise, is observed and has been shown to be caused by blade thickness and transonic effects. It is at a maximum near the tip-path plane of the rotor and falls off with increasing lateral directivity angles. As a consequence, the pilot cannot identify this large acoustic energy radiation from inside the helicopter. Furthermore, at high tip Mach numbers an extremely sharp positive pressure rise follows this sharp expansion wave, resulting in very intense radiated noise levels which indicate that this rapid increase in pressure is associated with a radiating shock wave.

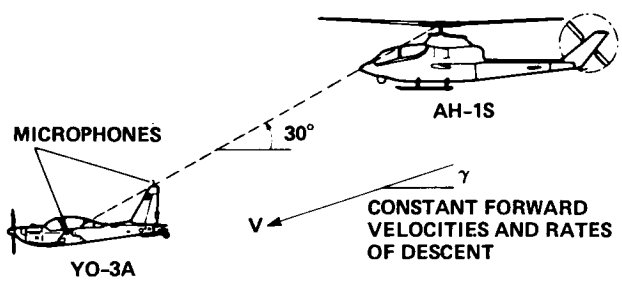


Figure 1.- In-flight technique.

In order to study more closely this interesting phenomenon of a sharp positive acoustic pressure rise observed in a full-scale flight test, both small-scale-model wind tunnel tests and hover tests have been carried out with the following questions in mind:

1. Can high-speed impulsive noise be scaled, and if so, what are the scaling parameters?

2. Can high-speed impulsive noise be scaled in hover (i.e., how important are the unsteady effects)?

3. How accurately can high-speed impulsive noise be predicted? What degree of modeling is required?

4. How does a local shock wave radiate to the acoustic far field?

In order to duplicate the full-scale acoustic phenomena with small-scale models, several wind tunnel tests were carried out in the Ames 7 × 10 ft wind tunnel, CEPRA-19 anechoic wind tunnel, and DNW anechoic wind tunnel. The typical comparison of acoustic data of a 1/7-scaled AH-1/OLS model in the DNW tunnel with AH-1 full-scale flight test data is shown in figure 2. Negative peak pressure levels and waveform shapes are plotted as a function of advancing tip Mach number, which has been proven to be the most important nondimensional parameter of high-speed impulsive noise. (Further comparison of model acoustic data in the DNW and CEPRA-19 wind tunnels with AH-1 full scale flight test data can be found in refs. 2-4.) From the comparisons, it is clear that high-speed impulsive noise can be scaled and that the primary scaling parameters are geometry and the advancing tip Mach number.

The interesting aspect of high-speed helicopter noise is the development of the saw-toothed waveform at high advancing-tip Mach numbers as shown in figure 3. A near-symmetrical pulse is observed in case A ($M_T$ = 0.867), while the symmetrical pulse becomes saw-tooth in character (case B, $M_T$ = 0.9). This sudden change of the waveform is called delocalization and the corresponding tip Mach number is called the delocalization Mach number. This is a very unique phenomenon peculiar to a rotating blade, which will be discussed further in the later section. At still higher advancing tip Mach numbers (case C, $M_T$ = 0.925), the peak negative pressure becomes very large, and the sudden rise in pressure becomes nearly instantaneous. The noise generated by this latter waveform is rich in higher harmonics and can be subjectively classified as harsh and extremely intense. The exact same phenomena were also observed in hover as shown in figure 4 (details in ref. 5). The most remarkable observation about the model-hovering rotor data is their pulse shape similarity to the model-scale acoustic data taken in forward flight. Although the hovering amplitudes are higher than the forward flight amplitudes, the delocalization process is duplicated quite well. This implies that the unsteady aerodynamic effects of forward flight play a secondary role in the delocalization process. The high-speed impulsive noise signatures generated by full- and model-scale forward flight tests can be studied to first order in hover and the scaling parameter is the advancing tip Mach number.

The theoretical analysis is based on the well-known integral equation derived by Ffowcs Williams and Hawkings (ref. 6).

$$4\pi a_o^2 \rho'(\bar{x},t) = \frac{\partial}{\partial t}\int_S \left[\frac{\rho_o v_n}{r|1 - M_r|}\right] ds - \frac{\partial}{\partial x_i}\int_S \left[\frac{p_{ij} n_j}{r|1 - M_r|}\right] ds + \frac{\partial^2}{\partial x_i \partial x_j}\int_V \left[\frac{T_{ij}}{r|1 - M_r|}\right] d\bar{V} \tag{1}$$

Far-field acoustic pressure is explicitly expressed in terms of integrals over the blade surface (monopoles and dipoles) and over the surrounding volume (quadrupoles). A comparison between linear thickness calculations, first term in equation (1) versus the experimental data for hover, is shown in figure 5 for several different tip Mach numbers. The striking features of the comparison between theory

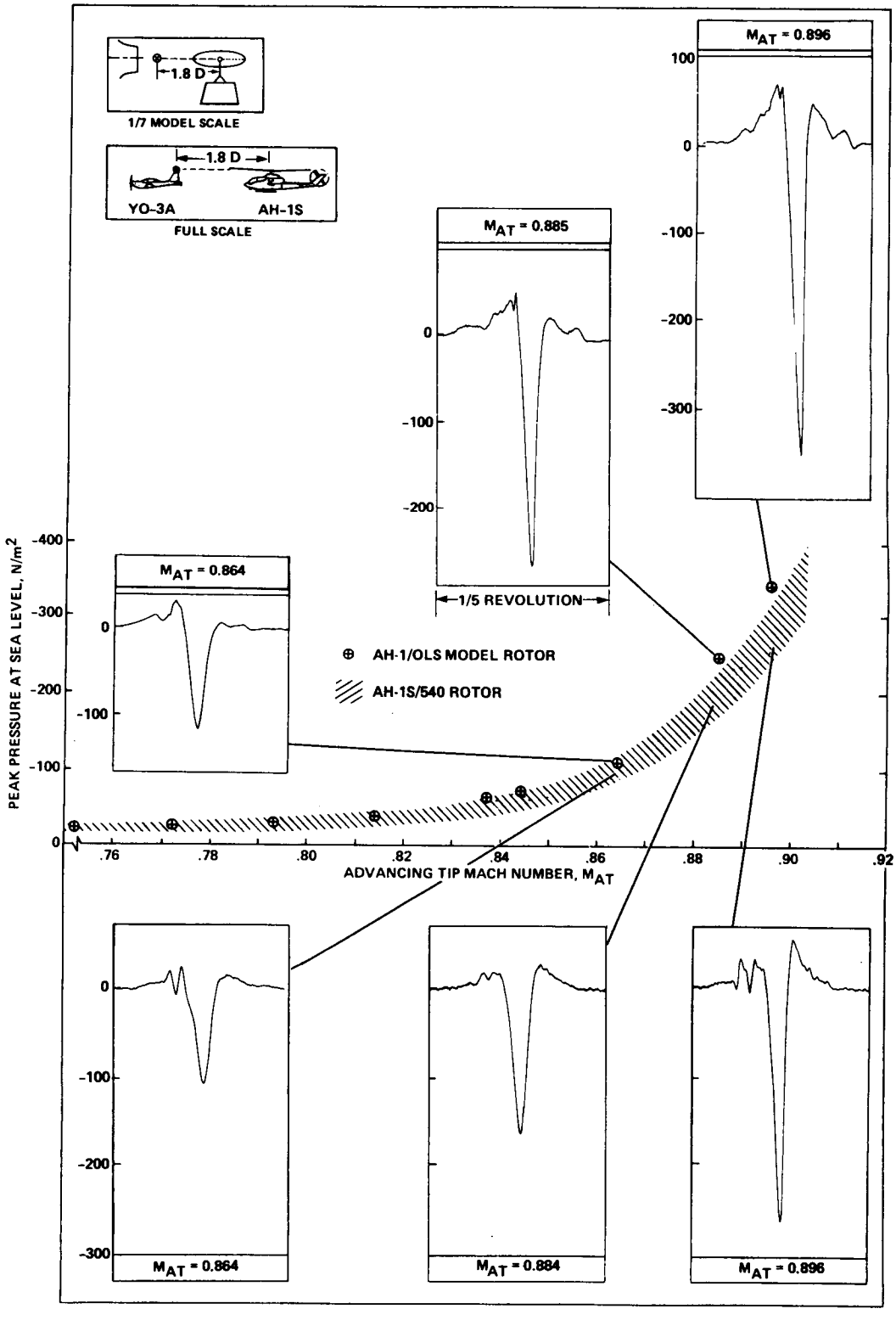


Figure 2.- Comparison of model and full-scale acoustic waveforms for an in-plane microphone 1.8 rotor diameters ahead.



C-7

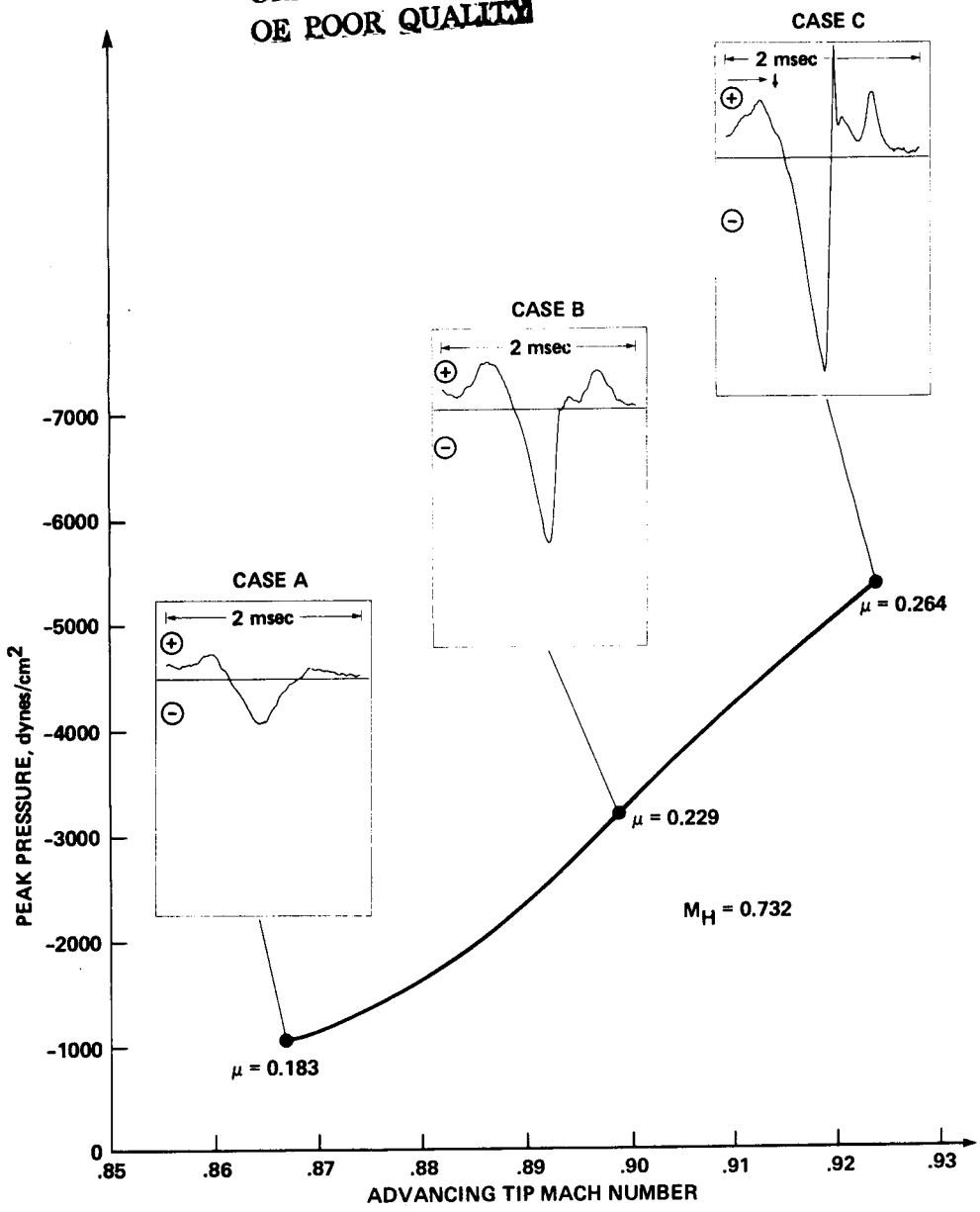


Figure 3.- Waveform shape versus advancing-tip Mach number.

and experiment at the tip Mach number less than 0.9 are the similarity in pulse shape and underprediction of the theory in negative peak levels by a factor of about 2. At hover tip Mach number of 0.9, the amplitude of the peak negative pressure pulse is again underpredicted by a factor of 2, but there is also a dramatic change in the waveform of the experimental data which is not predicted by the linear

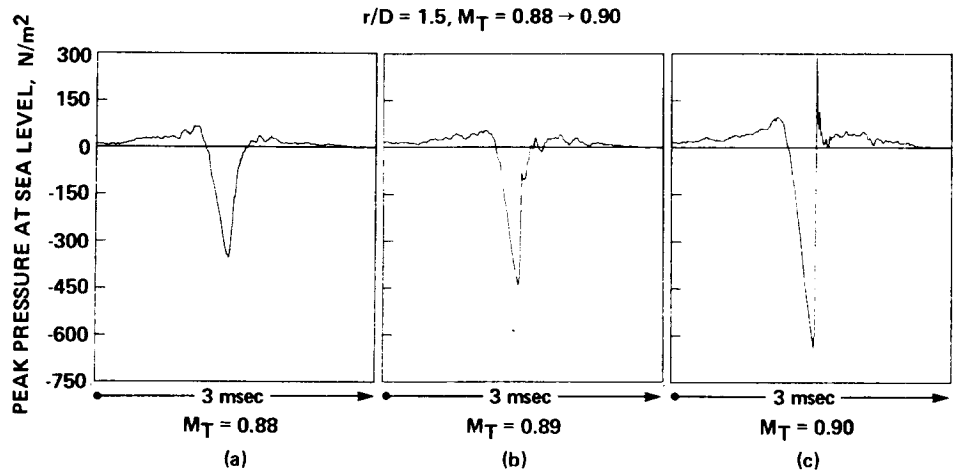


Figure 4.- Waveform transition; the development of a radiating discontinuity, in-plane, $r_H/D = 1.5$, $M_T = 0.90$.

theory.[1] The discrepancy between the linear theory and experimental data can be explained by nonlinear flow phenomena around the blade tip and can be lessened by adding the quadrupoles term of the governing equation. In order to incorporate the near aerodynamic nonlinear flow field into the quadrupole term of the equation, the governing potential equation was transformed (ref. 7) to blade-fixed cylindrical coordinates as follows:

$$\left\{\omega^2 - \frac{a_o^2}{r^2} - (\gamma + 1)\frac{\omega}{r^2}\phi_\theta\right\}\phi_{\theta\theta} - 2\omega\phi_r\phi_{r\theta} - 2\omega\phi_z\phi_{z\theta} = \{a_o^2 + (\gamma - 1)\omega\phi_\theta\}\left(\phi_{rr} + \frac{1}{r}\phi_r + \phi_{zz}\right) \qquad (2)$$

This transonic equation governs the delocalization phenomenon and also helps explain the influence of the transonic flow field on the acoustic far field signatures. The coefficient of $\phi_{\theta\theta}$ determines the propagation behavior of the local shock depending on its sign. Below the local sonic Mach number, the coefficient becomes a negative sign and the equation (2) behaves like an elliptic-type equation in which no wave-like behavior is possible. In this case, the local shock structure does not propagate into the acoustic far field. However, above a local sonic Mach

[1]The remaining linear dipole term [second term in the eq. (1)] was included in reference 8 and the results were almost indistinguishable from those of the monopole calculations. Also, similar conclusions were drawn in reference 9 for a high-speed rotor in forward flight. In addition, most of the experimental data suggested that the high-speed noise phenomenon was not dependent on thrust or torque at a constant Mach number.

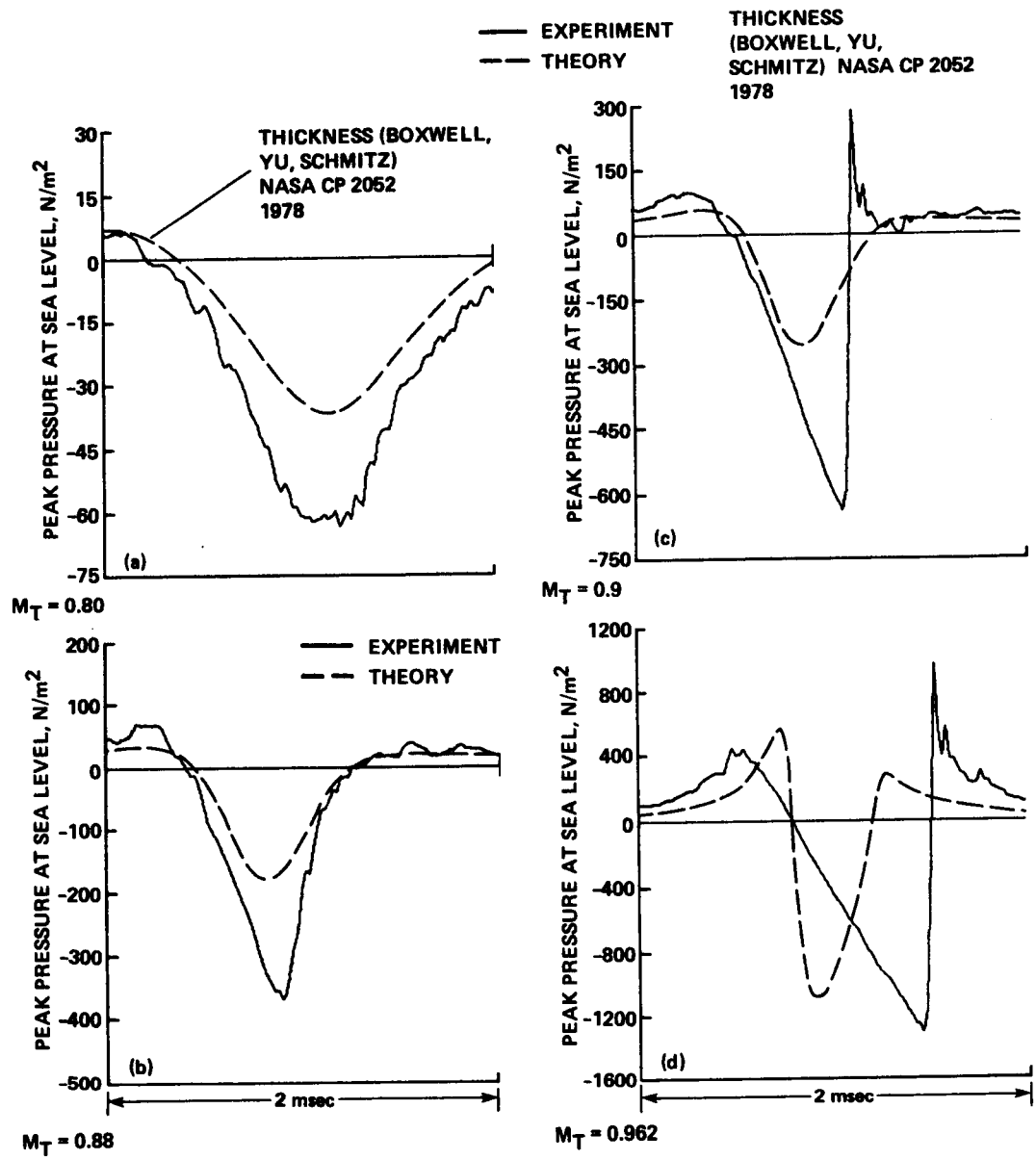


Figure 5.- Comparison of theory with experimental pressure time-history, in-plane, $r_H/D = 1.5$. (a) $M_T = 0.8$; (b) $M_T = 0.88$; (c) $M_T = 0.9$; (d) $M_T = 0.962$.

number, the coefficient becomes positive and equation (2) becomes hyperbolic. Local shock waves then propagate into the acoustic far field without interruption and generate strong shock characteristics in the acoustic signatures. This phenomenon is called the delocalization. Since this delocalization phenomenon is directly related to the acoustic far field, a logical step in the prediction of acoustic field is the incorporation of the near-field aerodynamic nonlinearities into the acoustic formulation. The accuracy of the acoustic far-field calculation is totally dependent on the detailed knowledge of the near-field aerodynamic nonlinearities surrounding the blade. The comparison of acoustic waveform calculations with a three-dimensional transonic numerical code (ref. 10) against the experimental data is shown in figure 6.

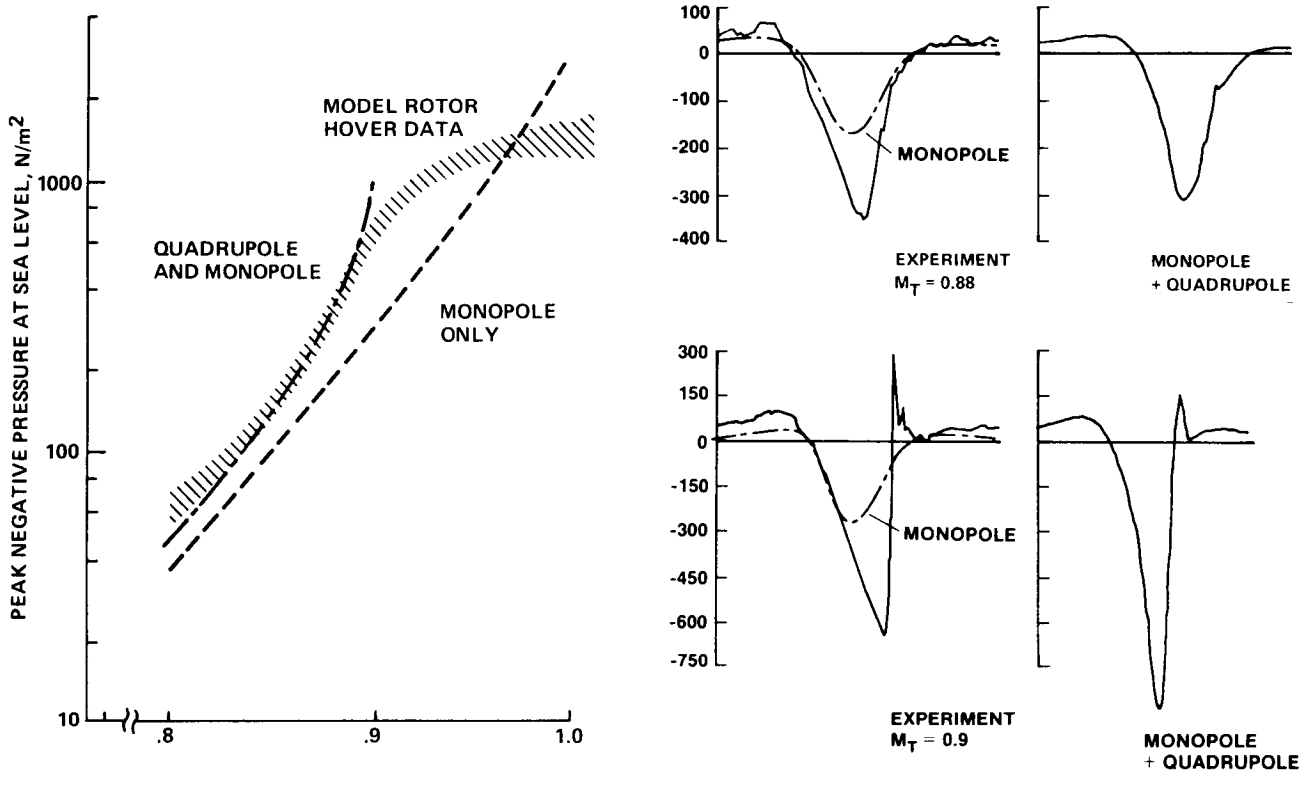


Figure 6.- Comparison of theory and experiment in hover, in-plane, r/D = 1.5.

At Mach numbers below the delocalization Mach number (0.9 for the NACA 0012 airfoil with a rectangular planform), the waveform shape is basically symmetrical and good correlation in amplitude and waveform shape is observed. At the tip Mach number of 0.90, the nonlinear quadrupole term changes waveform shape dramatically and increases in amplitude, leading to good agreement in pulse shape. This is a reflection of the fact that local shocks are propagating from the surface of the airfoil to the acoustic far field. However, in these comparisons, the amplitude is now overpredicted at or above a tip Mach number of 0.9 even though the waveform changes from the symmetric to saw-tooth shapes at the correct Mach number as shown in the experimental data. This has suggested several areas where improvements can be made, and they are discussed in the following sections.

The experimental verification of this computational code is less satisfactory because of a lack of high quality near-field experimental data. In order to improve this situation, a new experimental technique, called optical holographic interferometry/computerized tomography, has been developed. A powerful pulsed ruby laser recorded 40 interferograms with a 2-ft view field around the model rotor blade tip operating at a tip Mach number of 0.9 (see fig. 7). After digitizing interferograms and extracting fringe-order functions, the computerized tomography code reconstructed the flow field, providing pressure coefficient contours in several planes as shown in figure 8 (refs. 11-13). The results from this holographic technique give very good agreement with previously obtained numerical computations and laser

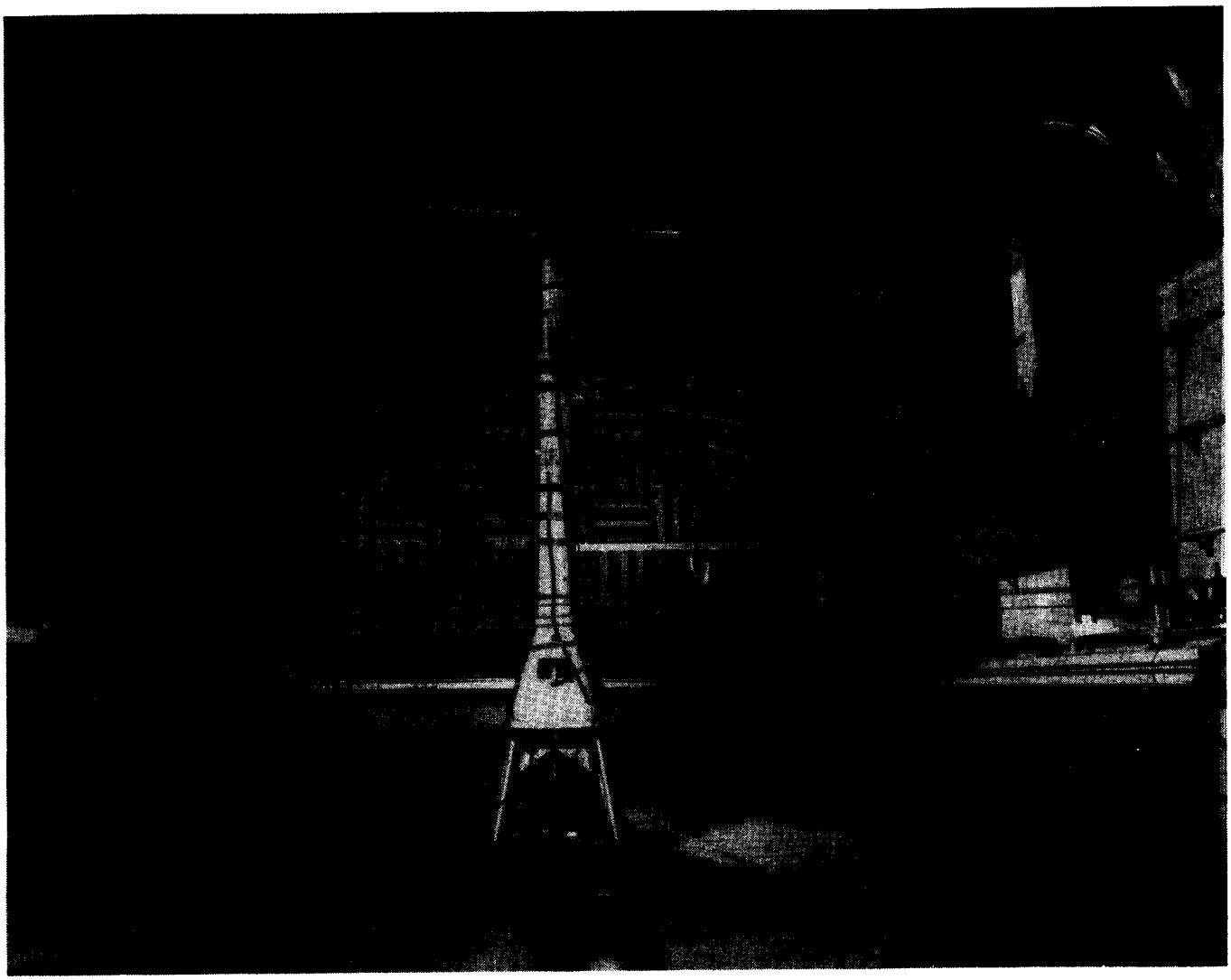

Figure 7.- Holographic interferometry setup.

velocimeter measurements of the aerodynamic flow field surrounding the rotor. Several important features of the holographic technique are (1) the lack of geometrical constraints in the optical system leads to the ability to conduct large-scale, nonlaboratory tests, (2) a single photo film contains a large volume of instantaneous three-dimensional flow information, providing a substantial reduction in test time, and (3) the reconstruction procedure can be performed in a laboratory, not in the test section where interferograms are recorded.

Therefore, the holographic technique with the computerized tomography proved to be a highly effective way to measure the large volume of the instantaneous three-dimensional, transonic flow field surrounding a rotor blade.

Another potential acoustic prediction method has been developed for the high-speed impulsive noise phenomenon using the methods of geometrical acoustics and computational fluid dynamics (CFD). With the geometrical acoustics approximation,

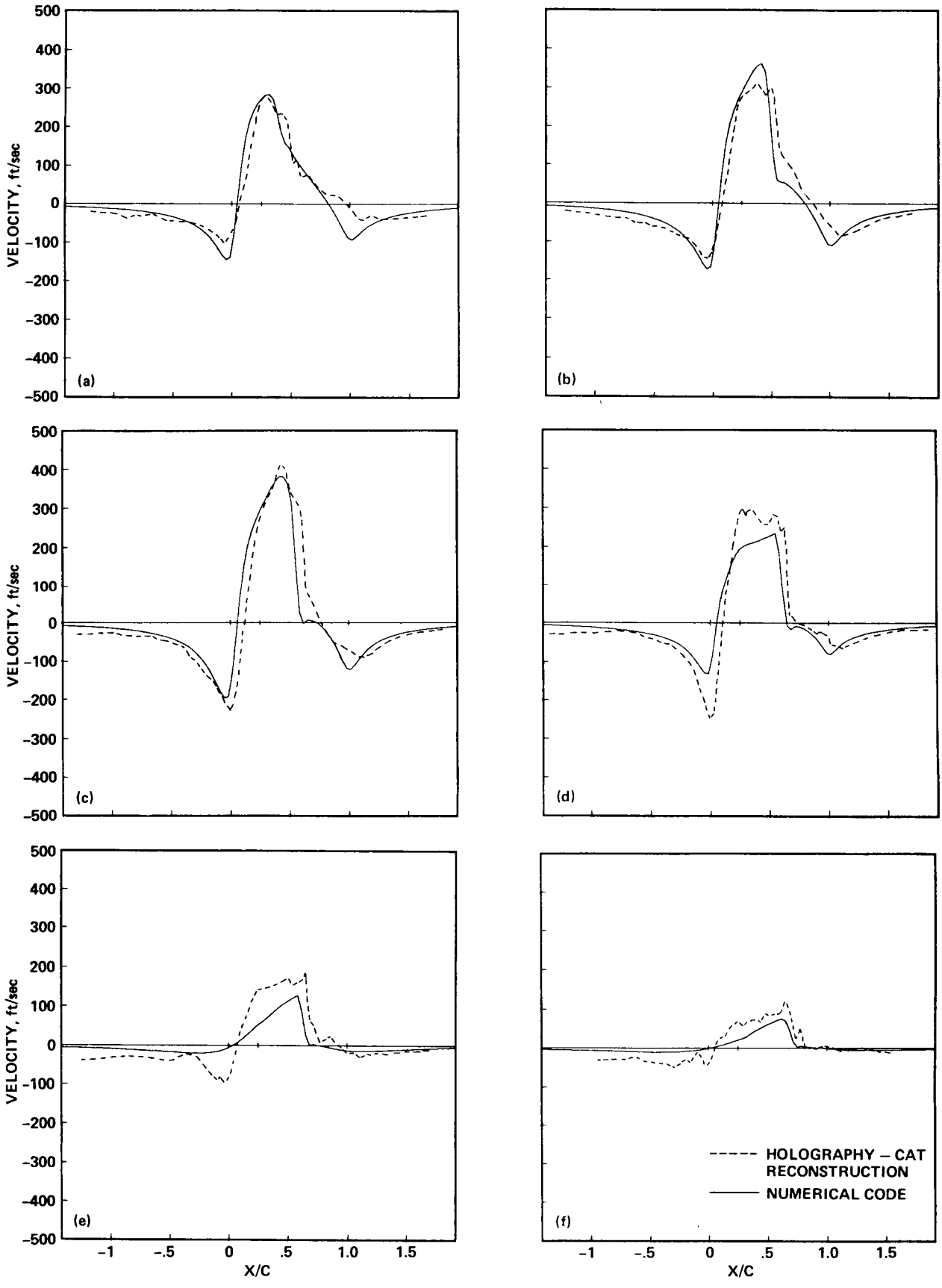


Figure 8.- Perturbation velocity distributions at six radial locations for Y/C = 0.8 above blade centerline. (a) $R/R_o$ = 0.88; (b) $R/R_o$ = 0.92; (c) $R/R_o$ = 0.96; (d) $R/R_o$ = 1.00; (e) $R/R_o$ = 1.04; (f) $R/R_o$ = 1.08.

the new Kirchhoff formula was developed by Isom (ref. 14), in which the quadrupole volume integral in the Ffowcs Williams and Hawkings formulation is reduced to a surface integral over the plane tangent to the sonic cylinder. Then, the initial data on the sonic cylinder are obtained from a transonic CFD code that solves the full potential equation in the near aerodynamic nonlinear field. Since CFD codes are less successful in the far field, this new approach combines the near-field aerodynamic calculation from a CFD code with the geometrical acoustic approximation in the acoustic far field (ref. 15).

## 3. BLADE-VORTEX INTERACTION (BVI) NOISE

The physical understanding of blade-vortex interaction noise is not as complete as is that of high-speed impulsive noise. Although there have been many experimental and theoretical efforts which have shown progress in understanding the generating mechanisms, only a few qualitative design changes have resulted. Similar to questions raised about high-speed impulsive noise, the following questions will be discussed:

1. Can BVI noise be scaled, and if so, what are the scaling parameters?

2. What are the known physical origins of BVI noise?

3. How accurately can BVI noise be predicted?

A comparison of the acoustic signatures of the Operational Loads Survey (OLS) model tests in both the CEPRA-19 and DNW anechoic wind tunnels with the 540 rotor full-scale flight test is shown in figure 9. A microphone is located approximately 30° beneath the plane of the rotor tips. This relative orientation of the microphone is known to maximize the blade-vortex interaction noise and reduce the magnitude of high-speed impulsive noise. The average time history of acoustic signatures from the model- and full-scale rotor systems become strikingly similar when the four important nondimensional scaling parameters are matched: advancing tip Mach number, advanced ratio, $C_{T/\sigma}$, tip-path-plane angle. (A more complete picture of the comparison of model- and full-scale blade vortex interaction noise is shown in ref. 16.) Good general agreement in amplitude as well as pulse shapes between model- and full-scale tests is apparent at all descent conditions at low advance ratios ($\mu \leq 0.2$). At high advance ratios, the BVI phenomenon was not well scaled. The reasons for this are not known at the present time.

There were several tests performed to simultaneously measure the acoustic and aerodynamic field so that the aerodynamic data could be used as input to acoustic prediction codes. A major full-scale experiment was carried out by a joint U.S. Army/Bell Helicopter program, called the Operational Loads Survey (OLS). Several small scale OLS-model wind tunnel tests were also performed in the 14 × 22 Foot Wind Tunnel (ref. 17) and CEPRA-19 and DNW anechoic wind tunnels (refs. 18 and 19). From these tests, one of the most important findings was that the BVI phenomenon was seen to be concentrated near the very leading edge of the blade chord. Furthermore, the

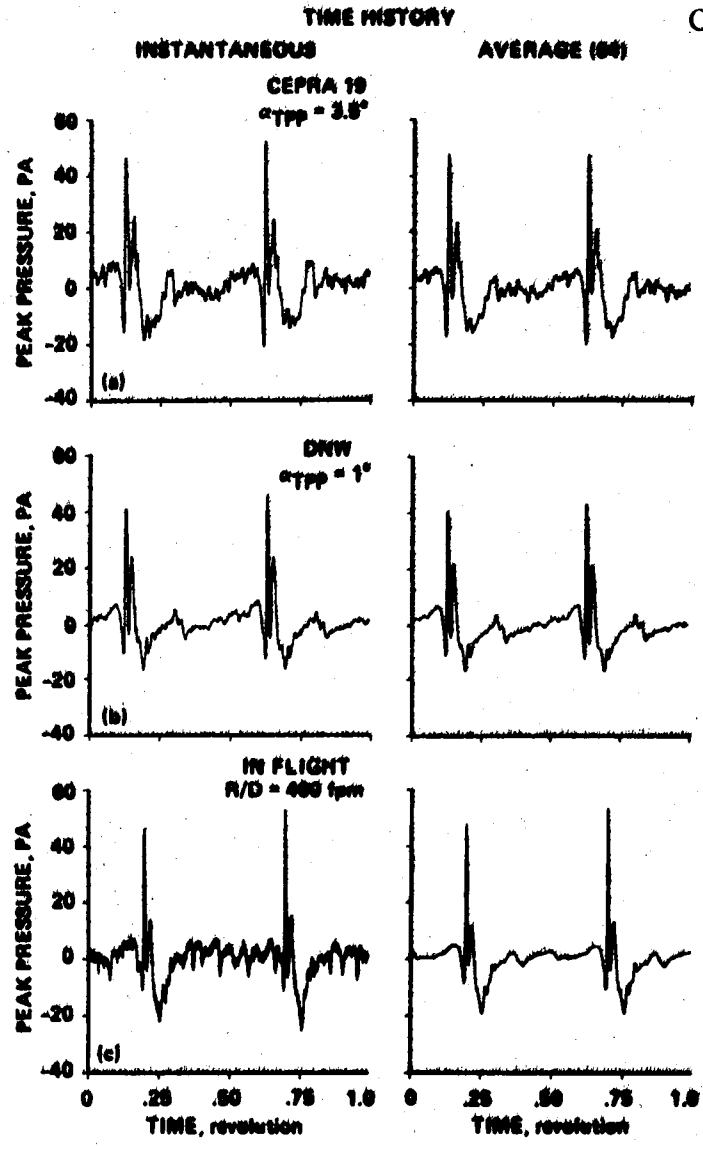


Figure 9.- Rotor acoustic comparisons, 30° below rotor-plane microphone: $\mu$ = 0.164, $M_{AT}$ = 0.772, $C_T$ = 0.0054. (a) CEPRA 19 time-history, $\alpha_{TPP}$ = 3.5°; (b) DNW time-history, $\alpha_{TPP}$ = 1.0°; (c) full-scale time-history, R/D = 400 ft/min.

interaction of 3/2 revolution old vortex and the blade in the advancing side appears a strong contributor on the acoustic field, in which the vortex and the blade are positioned almost parallel. Because of the local transonic flow around the leading edge generated by the nearby vortex, the near-discontinuous acoustic pressure propagation was observed in some Schlieren pictures of advancing-side BVI on a small-model rotor in a wind tunnel (ref. 20).

To predict the acoustic pressure measurements, equation (1) can be used where only the pressure term (acoustic dipole sources) is used. A computer model of the BVI phenomenon from the measured pressure data was constructed which carefully fit the measured data and kept track of the interaction loci. The comparison of the

measured OLS and computed acoustic waveforms are shown in figure 10 (ref. 21). The general waveform was well predicted in the right wing and nose-boom microphones; however, the peak amplitudes are underestimated and the pulse widths overestimated. These discrepancies may be traced to experimental frequency response limitations of the data measurement system, analytical modeling of the measured pressure data, or possibly to the omission of quadrupole sources caused by transonic flow.

Based on the model- and full-scale experiments, it is thought that compressibility plays a significant role in the aerodynamics of BVI. The local transonic flow field which exists during BVI has initially been simplified to a two-dimensional (2-D) encounter with the vortex passing by a stationary airfoil. The governing computational fluid dynamic (CFD) equations are then numerically solved to yield both the aerodynamic forces and the radiated noise. The transonic small disturbance equation was used with a concentrated potential (irrotational) vortex structure to investigate the unsteady pressure fluctuation on the airfoil surface and the propagation of acoustic waves to the far field. The propagating wave and its structure is clearly visible in figure 11 where much more energy is seen to propagate in the upstream direction (ref. 22). It is clear that the computational technique can be used to gain insight into the highly complex nonlinear blade vortex interaction phenomena.

In order to validate computational codes and to improve the physical understanding, other experimental techniques are being developed under the Army supervision to help understand the basic mechanisms of BVI. In one such experiment, an airfoil was placed in a shock tube in the wake of a vortex generator in which the 2-D airfoil-vortex interaction phenomenon was simulated. The event was measured with pressure transducers, high-speed Mach-Zehnder interferometry (ref. 23), and holographic interferometry (ref. 24).

This pioneering computational and experimental work is in the beginning stages of development. These preliminary results are encouraging and reaffirm the importance of leading-edge blade geometry on the BVI problem. In the near future, this work should be able to suggest leading-edge geometries that tend to minimize the airfoil pressure disturbances leading to generation of less BVI acoustic energy that is radiated to the far field.

Because of the importance of the trailing tip vortex strength, blade tip planform should have an important effect on BVI noise. A test was carried out in the NASA Langley 14 × 22 Foot Wind Tunnel to evaluate the potential benefits of tip-shape modification in alleviating blade-vortex interaction noise as shown in figure 12. The results of the program (ref. 25) showed that a tip shape can be designed such that a modest improvement can be achieved in the blade-vortex interaction noise propagation characteristics as compared to a rectangular tip shape. Furthermore, a test program of an advanced blade design for the Army's UH-1 helicopter fleet was also carried out in the 14 × 22 Foot Wind Tunnel to determine the performance benefits provided by rotor blade planform taper as shown in figure 13. It appeared that the advanced rotor design did not significantly reduce the blade-vortex interaction noise, while high-speed impulsive noise could be reduced substantially (about 8 or 9 dB reduction) (refs. 26 and 27).

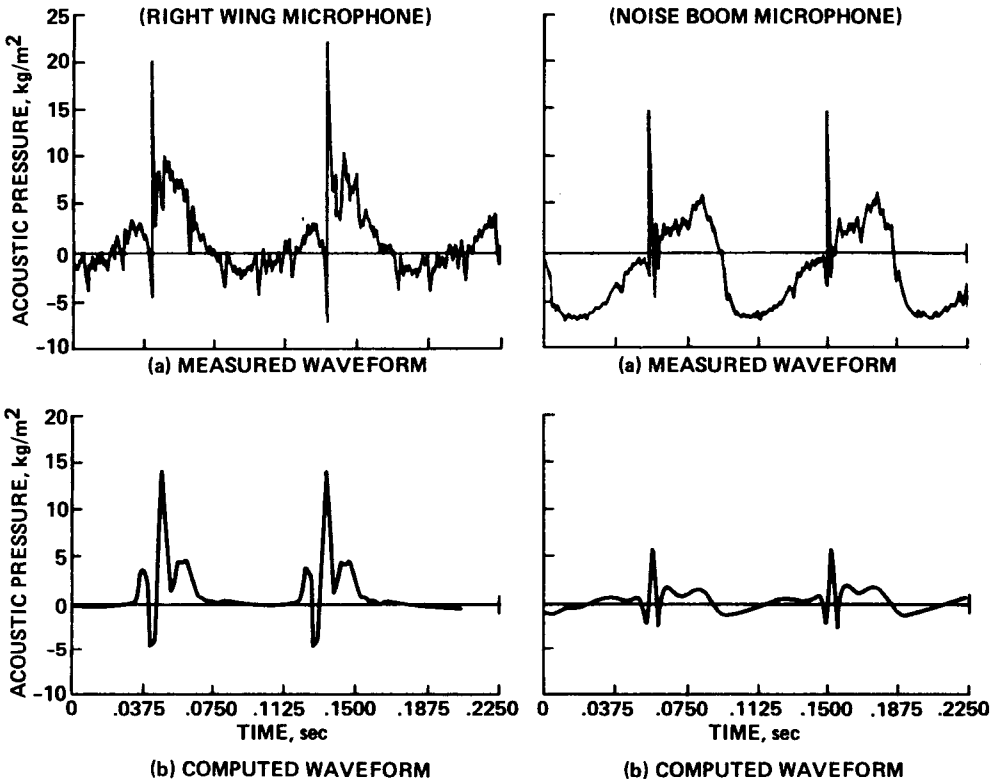


Figure 10.- Comparison of acoustic waveform between measurement and computation.

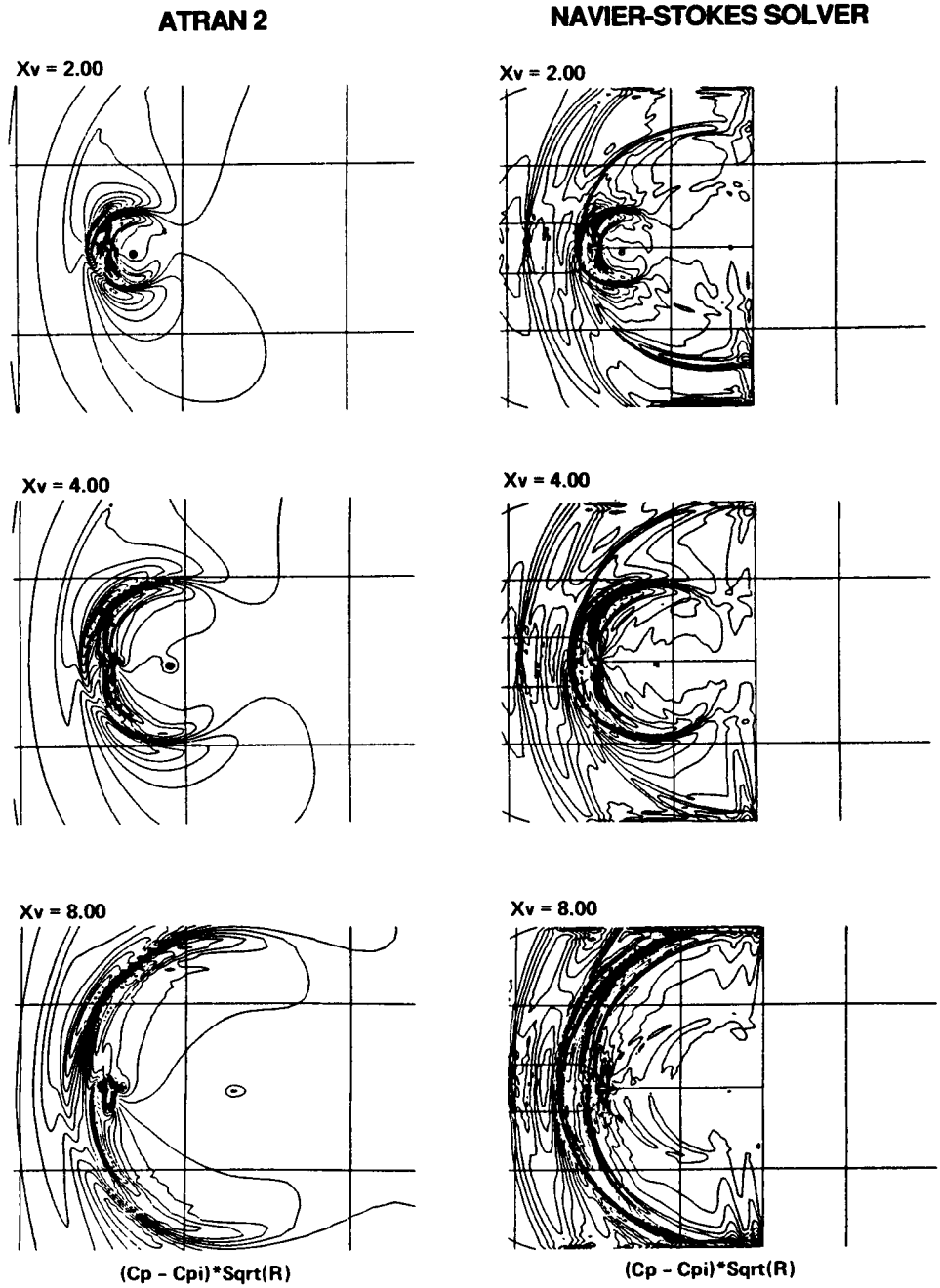


Figure 11.- Wave propagation due to blade-vortex interaction.

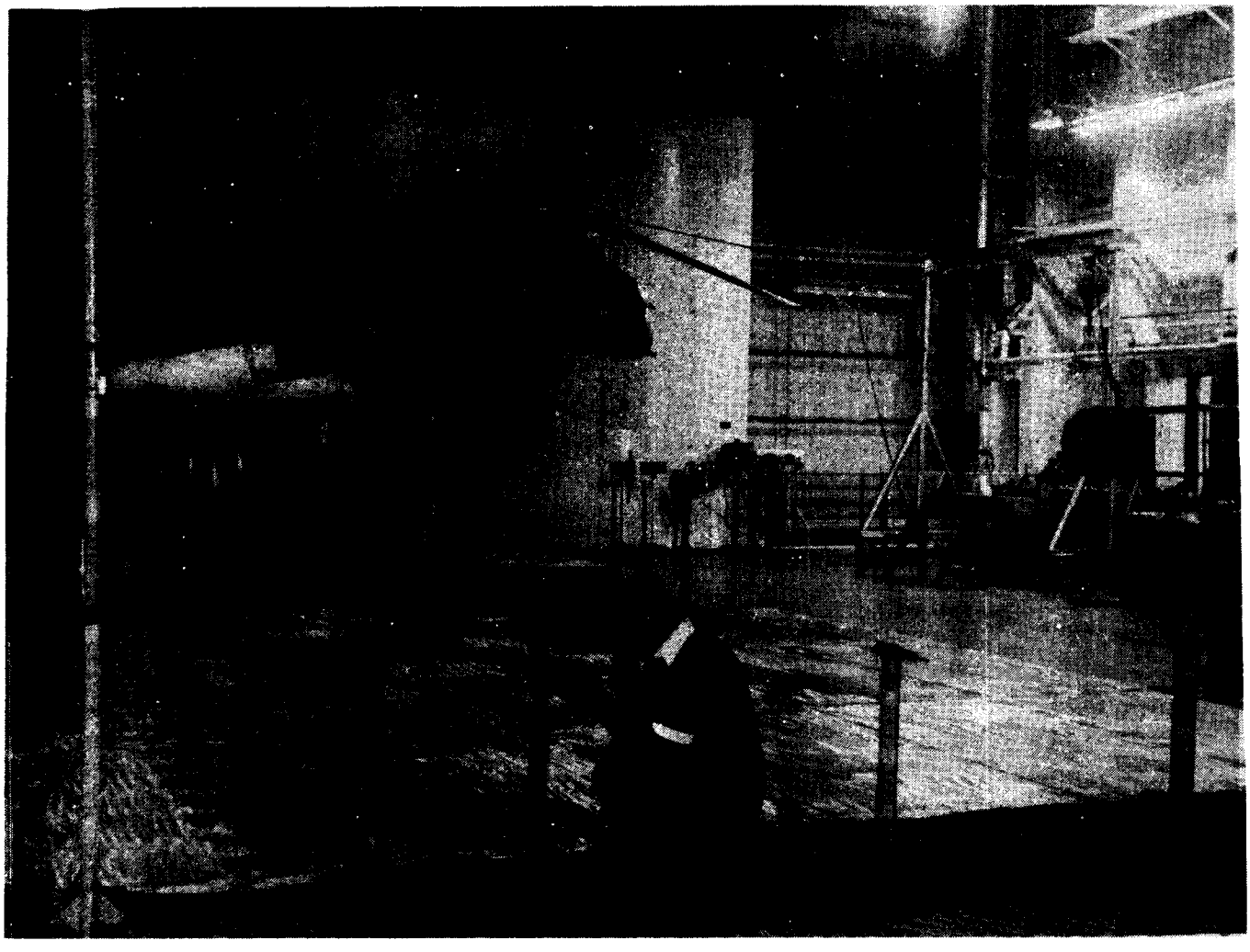

Figure 12.- UH-1 acoustic test at NASA Langley 14 × 22 Foot Wind Tunnel.

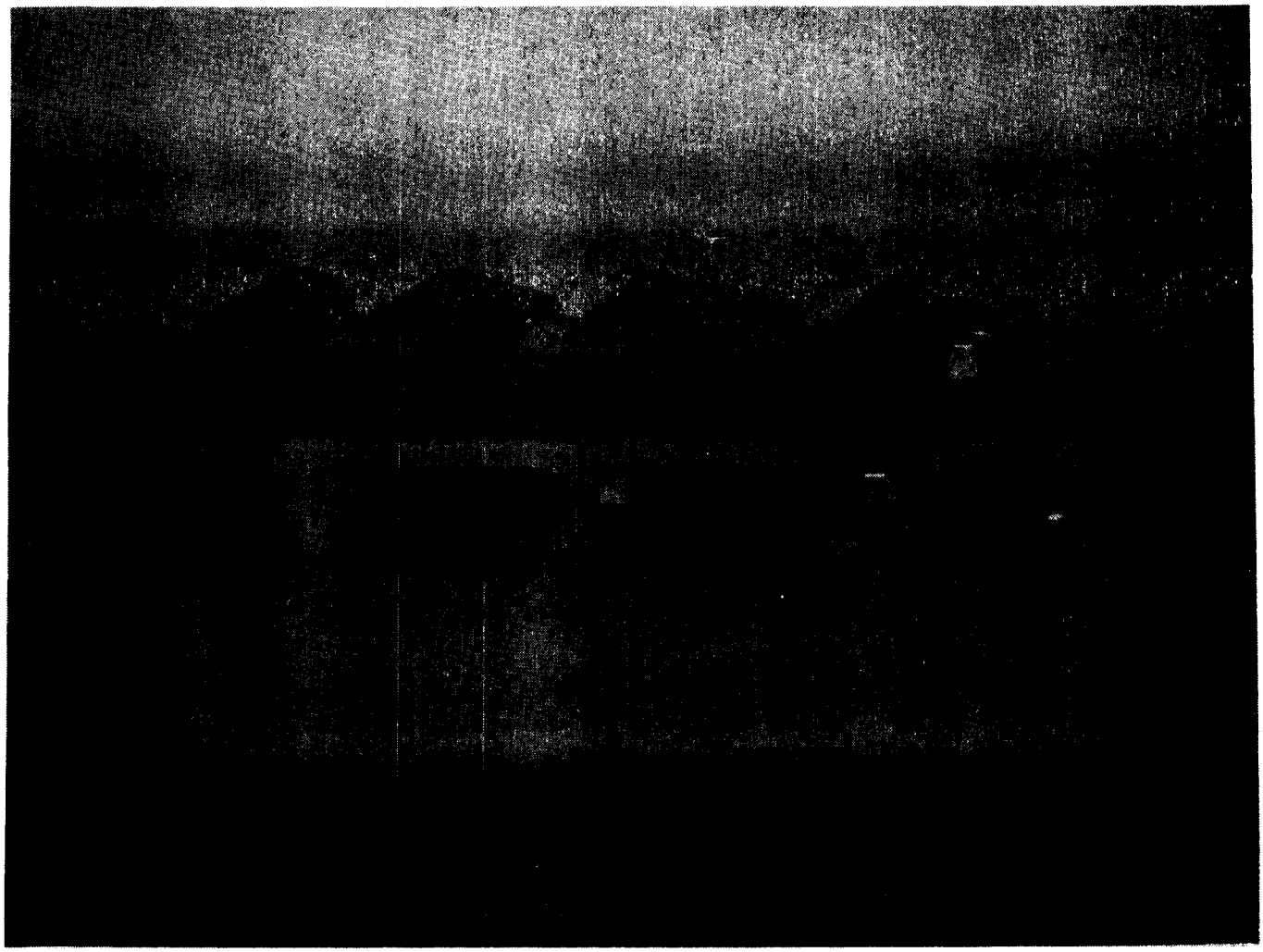

Figure 13.- Tip-shape generic rotor test.

## 4. ACOUSTIC AND AERODYNAMIC TEST OF A MODEL ROTOR (AATMR) PROGRAM

A new joint program between the Army and the rotorcraft industry has been initiated to take acoustic and aerodynamic measurements in the DNW wind tunnel with advanced, dynamically scaled, pressure instrumented model rotor systems to relate the important aerodynamic phenomena to the near- and far-field acoustic radiation. In particular, high-speed impulsive noise, blade-vortex interaction noise, and low-frequency harmonic noise are being studied. Particular test objectives are (1) to verify existing analytical prediction codes for acoustics and aerodynamics with dynamically flexible blades, (2) to compare the measured data with full-scale flight data and full-scale wind tunnel data and develop scaling parameters, and (3) to improve blade design capabilities.

A first test was performed this past summer under a joint research agreement with the Aeroflightdynamics Directorate (ARTA) and Boeing Vertol. Boeing Vertol furnished a 1/5 dynamically scaled, pressure instrumented model of the BV 360 rotor in the DNW wind tunnel (fig. 14) which was tested by the Army/Boeing-Vertol with NASA's assistance. During the test, the on-line digital data acquisition and processing system gathered extremely accurate acoustic and pressure signatures of the rotor. In addition, very low-speed shadowgraph photographs were taken to define the epicycloid patterns of tip vortex trajectories and a photogrammetry technique was also attempted to measure the live twist distributions of the highly elastic BV 360 rotor blades. The data reduction process is under way and results will be available shortly (ref. 28).

## 5. CONCLUDING REMARKS

This paper reviews the progress made in helicopter aerodynamically generated impulsive noise by Army researchers over the past decade. From full-scale flight tests and several small-scale model wind tunnel tests, it is clear that high-speed impulsive noise can be scaled and the primary scaling parameter is the advancing tip Mach number. Also improved basic physical understanding of the high-speed impulsive noise generating mechanism and of the delocalization phenomenon has been substantially achieved for use in the design of advanced blades for reduced noise. In the case of blade-vortex interaction (BVI) noise, the physical understanding of the noise generating mechanism is not as complete as that of high-speed impulsive noise. However, the BVI noise can be scaled for low advance ratios and the scaling parameters are advancing tip Mach number, advanced ratio, $C_{T/\sigma}$, and tip-path-plane angle. Because of the compressibility effect on BVI aerodynamics, CFD techniques are now emerging for understanding the basic mechanisms of BVI and the associated radiated noise mechanisms. The preliminary results are very encouraging and CFD techniques should help to design a blade for reduced noise. The cooperative programs between the Army, NASA, and industry have been very successful and will be continued.

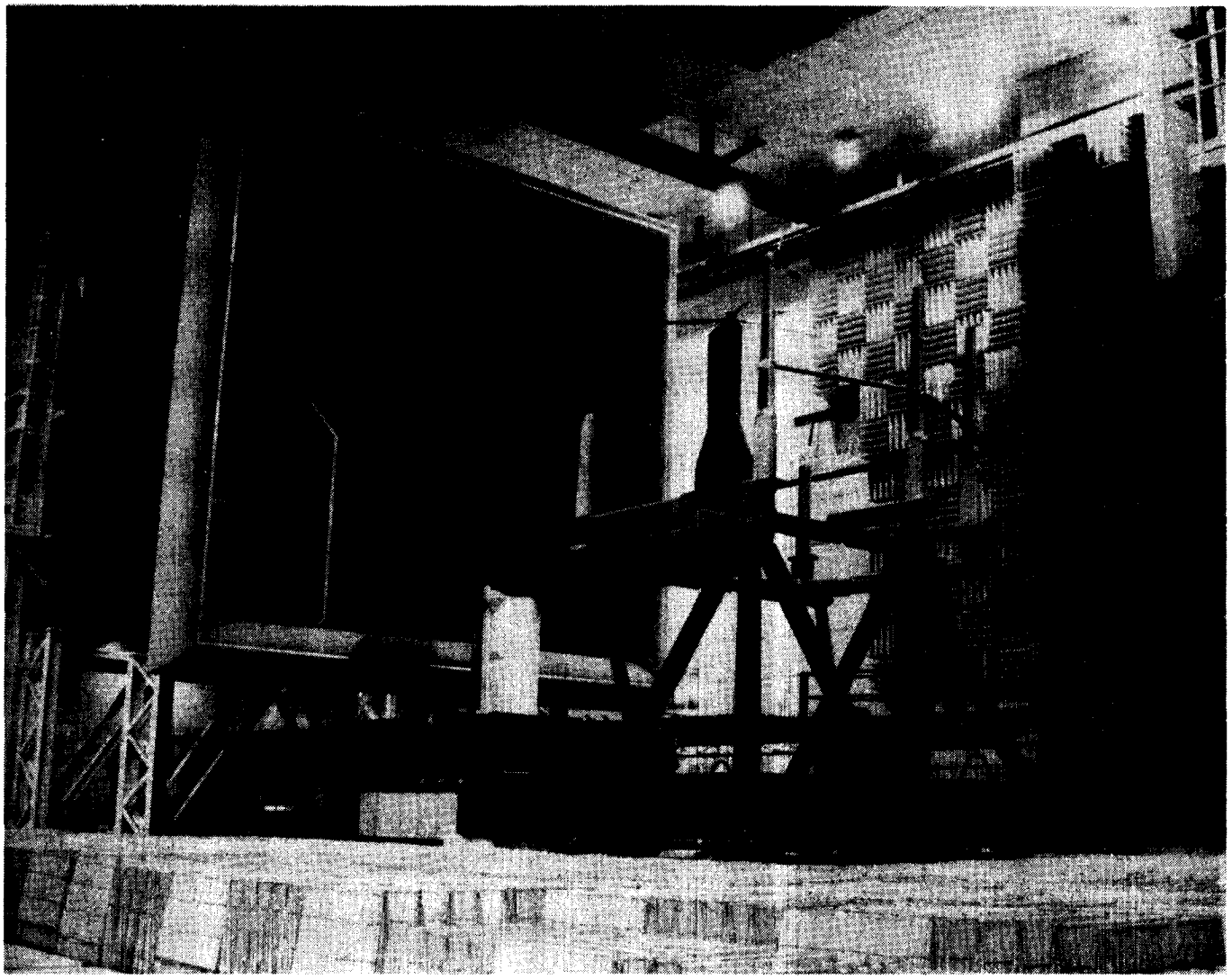

Figure 14.- BV-360 rotor system at the DNW wind tunnel.

## 6. ACKNOWLEDGMENTS

The authors wish to acknowledge support and contributions of our many friends and colleagues at the Aeroflightdynamics Directorate and Aerostructures Directorate; in particular, Mr. Andrew W. Kerr, Director; Mr. Donald Boxwell; Dr. Francis Caradonna; Mr. Danny Hoad; and Professor Morris Isom. Also, sincere appreciation goes to our many colleagues at the U.S. Army Research Office (ARO), ONERA, DNW, DFVLR, NLR, NASA, and U.S. helicopter manufacturers for their talents and enthusiastic support.

## 7. REFERENCES


1. Schmitz, F. H.; and Boxwell, D. A.: In-Flight Far-Field Measurement of Helicopter Impulsive Noise. Journal of the American Helicopter Society, vol. 21, 1976, pp. 2-16.

2. Boxwell, D. A.; Schmitz, F. H.; Splettstoesser, W. R.; Schultz, K. J.; Lewy, S.; and Caplot, M.: A Comparison of the Acoustic and Aerodynamic Measurements of a Model Rotor Tested in Two Anechoic Wind Tunnels. NASA TM 88364, 1986.

3. Splettstoesser, W. R.; Schultz, K. J.; Schmitz, F. H.; and Boxwell, D. A.: Model Rotor High-Speed Impulsive Noise--Parametric Variations and Full-Scale Comparisons. Presented at the 39th Annual Forum of the American Helicopter Society, May 1983.

4. Boxwell, D. A.; Schmitz, F. H.; Splettstoesser, W. R.; and Schultz, K. J.: Model Helicopter Rotor High-Speed Impulsive Noise: Measured Acoustics and Blade Pressures. Presented at the Ninth European Rotorcraft Forum, Paper 17, Stresa, Italy, Sept. 1983.

5. Boxwell, D. A.; Yu, Y. H.; and Schmitz, F. H.: Hovering Impulsive Noise: Some Measured and Calculated Results. Vertica, vol. 3, 1978, pp. 35-45.

6. Ffowcs Williams, J. E.; and Hawkings, D. L.: Philosophical Transactions of the Royal Society London, Series A, vol. 264, 1969, pp. 321-342.

7. Isom, M. P.: Some Non-Linear Problems in Transonic Helicopter Acoustics. Report 79-19, Department of Mechanical and Aerospace Engineering, Polytechnic Institute of New York, 1979.

8. Farassat, F.; Nystrom, P. A.; and Morris, C. E. K.: A Comparison of Linear Acoustic Theory with Experimental Noise Data for a Small Scale Hovering Rotor. Paper 79-0608, AIAA Aeroacoustic Conference, Seattle, Washington, 1979.

9. Schmitz, F. H.; and Yu, Y. H.: Helicopter Impulsive Noise: Theoretical and Experimental Status. Journal of Sound and Vibration, vol. 109, no. 3, 1986, pp. 361-422.

10. Caradonna, F. X.: The Transonic Flow on a Helicopter Rotor. Ph.D. dissertation, Dept. of Aeronautics and Astronautics, Stanford University, 1978.

11. Yu, Y. H.; and Kittleson, J. K.: Reconstruction of a Three-Dimensional Transonic Rotor Flow Field from Holographic Interferograms. AIAA Journal, vol. 25, no. 2, Feb. 1987, pp. 300-305.

12. Becker, F.; and Yu, Y. H.: Digital Fringe Reduction Techniques Applied to the Measurements of Three-Dimensional Transonic of Flow Fields. Optical Engineering, vol. 24, no. 3, May/June 1985, pp. 429-434.

13. Kittleson, J. K.; and Yu, Y. H.: Transonic Rotor Flow-Measurement Technique Using Holographic Interferometry. Journal of American Helicopter Society, Oct. 1985, pp. 3-10.

14. Isom, M. P.: Geometrical Acoustics and Transonic Helicopter Noise. Annual Contract Report, NASA Ames Contract NCC 2-172, 1987.

15. Purcell, T. W.; Strawn, R. C.; and Yu, Y. H.: Prediction of High-Speed Rotor Noise with a Kirchhoff Formula, presented at the AHS Specialists' Meeting on Aerodynamics and Aeroacoustics, Arlington, Texas, 1987.

16. Boxwell, D. A.; and Schmitz, F. H.: Full-Scale Measurements of Blade-Vortex Interaction Noise. Paper 80-61, presented at the 36th Annual Forum of the American Helicopter Society, Washington, D.C., May 1980.

17. Hoad, D. R.; and Greene, G. C.: Helicopter Noise Research at the Langley V/TOL Tunnel, NASA CP-2052, 1978.

18. Splettstoesser, W. R.; Schultz, K. J.; Boxwell, D. A.; and Schmitz, F. H.: Helicopter Model Rotor-Blade Vortex Interaction Impulsive Noise: Scalability and Parametric Variations. Paper 18, presented at the Tenth European Rotorcraft Forum, The Hague, The Netherlands, Aug. 1984.

19. Schmitz, F. H.; Boxwell, D. A.; Lewy, S.; and Dahan, C.: A Note on the General Scaling of Helicopter Blade-Vortex Interaction Noise. Presented at the 38th Annual National Forum of the American Helicopter Society, 1982.

20. Tangler, J. L.: Schlieren and Noise Studies of Rotors in Forward Flight. Paper 77, presented at the 33rd Annual National Forum of the American Helicopter Society, Washington, D.C., 1977.

21. Nakamura, Y.: Prediction of Blade-Vortex Interaction Noise from Measured Blade Pressure. Presented at the Seventh European Rotorcraft and Powered Lift Aircraft Forum, Partenkirchen, Garmisch, Germany, 1981.

22. Baeder, J. D.; McCroskey, W. J.; and Srinivasan, G. R.: Acoustic Propagation Using Computational Fluid Dynamics. Presented at the 42nd Annual Forum of the American Helicopter Society, Washington, D.C., June 1986.

23. Meier, G. E. A.: Transonic Noise Generation by Duct and Profile Flow. Technical Report, Max Planck Institut fur Stromungsforschung, Gottingen, Germany, 1984.

24. Mandella, M.; and Bershader, D.: Quantitative Study of the Compressive Vortex: Generation, Structure and Interaction with Airfoils. Presented at the AIAA Aerospace Science Meeting, Reno, Nev., Jan. 1987.

25. Hoad, D. R.: Helicopter-Model Scale Results of Blade-Vortex Interaction Impulsive Noise as Affected by Tip Modifications. Paper 80-62, presented at the AHS 36th Annual Forum, Washington, D.C., 1980.

26. Hoad, D. R.: Evaluation of Helicopter Blade Vortex Interaction Noise for Five Tip Configuration. NASA TP 1608, 1979.

27. Martin, R. M.; Elliot, J. W.; and Hoad, D. R.: Comparison of Experimental and Analytic Predictions of Rotor Blade-Vortex Interactions Using Model Scale Acoustic Data. Paper 84-2269, presented at the AIAA/NASA 9th Aeroacoustics Conference, Williamsburg, Va., Oct. 1984.

28. Dadone, L.; Dawson, S.; Boxwell, D. A.; and Ekquist, D.: Model 360 Rotor Test at DNW---Review of Performance and Blade Airload Data. Presented at the 43rd Annual Forum of the American Helicopter Society, St. Louis, Mo., May 1987.